Magnetism and electronic structure of hcp Gd and the Gd(0001) surface

2002 J. Phys.: Condens. Matter 14 6353

(http://iopscience.iop.org/0953-8984/14/25/305)

INSTITUTE OF PHYSICS PUBLISHING JOURNAL OF PHYSICS: CONDENSED MATTER

J. Phys.: Condens. Matter **14** (2002) 6353–6371 PII: S0953-8984(02)33216-8

Magnetism and electronic structure of hcp Gd and the Gd(0001) surface

Ph Kurz, G Bihlmayer and S Blügel[1]

Institut für Festkörperforschung, Forschungszentrum Jülich, D-52425 Jülich, Germany

E-mail: G.Bihlmayer@fz-juelich.de

Received 30 January 2002
Published 14 June 2002
Online at stacks.iop.org/JPhysCM/14/6353

Abstract

We investigate hcp Gd and the Gd(0001) surface on the basis of density functional theory. The localized 4f states of Gd, which represent a challenge for first-principles theory, are treated in four different models, employing consistently the full-potential linearized augmented plane-wave method. Our results support previous findings that within the local density approximation (LDA) or generalized gradient approximation (GGA) the itinerancy of the 4f states is overestimated. In particular, the large density of states at the Fermi energy due to the minority 4f electrons is unphysical, and our results show that this is the origin of the incorrect prediction of the antiferromagnetic ground state for hcp Gd by many LDA and GGA calculations. We show that different models of removing these states from the region close to the Fermi energy, for example the treatment of the 4f electrons as localized core electrons or by using the LDA + U formalism, lead to the prediction of the correct ferromagnetic ground state for the bulk and a ferromagnetically coupled (0001) surface layer. With these models ground-state properties such as the magnetic moment and structural parameters can be determined in good agreement with experiment. The energetic positions of the surface states of the Gd(0001) surface are compared with experimental data.

(Some figures in this article are in colour only in the electronic version)

1. Introduction

The rare-earth metals are distinguished by their unique magnetic, electric and optical properties. They are of great practical interest because of their role in hard magnetic intermetallics [1] and high-density storage media [2]. The rare-earth metals are strongly correlated materials. The open shell of highly localized 4f electrons is responsible for their large magnetic moments.

[1] Permanent address: Fachbereich Physik, Universität Osnabrück, D-49069 Osnabrück, Germany.

0953-8984/02/256353+19$30.00

The overlap with the 4f shells on neighbouring lattice sites is negligible. Therefore, the 6s, 6p and 5d states play an essential role in the magnetism, because they mediate the magnetic interaction by a Ruderman–Kittel–Kasuya–Yosida- (RKKY-) type exchange, although their contribution to the magnetic moment is small. This complicated coupling mechanism leads to exotic magnetically ordered structures such as helical spin structures [3, 4]. Due to their localized f electrons that lie in the same energy range as the itinerant s, p and d electrons, they represent a challenge for first-principles theory.

In particular Gd, one of the four ferromagnetic (FM) elementary metals (Fe, Co, Ni and Gd) known to occur in nature, has been studied intensively by experiment and theory. It has become a model system for the application of new relativistic theoretical methods [5–7], because of the unique combination of ferromagnetism and relativistic effects. Experimentally many of the magnetic properties of Gd metal are well understood. The half-filled 4f shell ($S = 7/2$, $L = 0$) leads to the formation of a well localized spin-only magnetic moment. These moments couple via a RKKY-type exchange to form an FM Heisenberg system with a bulk Curie temperature of $T_C^B = 293$ K. The f-electron moment polarizes the valence electrons, resulting in a magnetic moment of 7.63 μ_B. However, the appropriate treatment of the localized 4f electrons in first-principles calculations is still a matter of debate. Several approaches have been suggested in addition to the treatment of the 4f bands as valence states, including the treatment as core states, the application of Hartree–Fock exchange [8–10] and the LDA + U model [11, 12].

The 4f-core model has already been introduced in a very early study [13]. Within the 4f-core model the 4f electrons are treated as core states, i.e. hybridization of the 4f states with other (valence) states and also with any states from other lattice sites is neglected. Much later Sticht and Kübler [6] performed self-consistent calculations in the local density approximation (LDA) comparing the 4f-core model and the 4f-band model, where the 4f electrons are treated as valence states. They obtained a much larger value for the magnetic moment (8.43 μ_B) from their 4f-core model calculation and concluded that this model was not an acceptable approximation. However, the large magnetic moment has not been reproduced by later 4f-core model calculations (e.g. [14]). From their 4f-band model calculation, Sticht and Kübler found a magnetic moment of 7.52 μ_B, in better agreement with experiment. By a comparison of the density of states (DOS) at the Fermi energy, $N(E_F)$, with specific-heat experiments they found that the calculated DOS was too large. They noted that the subtraction of the 4f contribution to the DOS resulted in a much better agreement. They also remarked that the binding energy of the majority 4f states was too small (4.5 eV) compared with photoemission data. Singh [15] carried out a detailed study using the 4f-band model, also finding that the DOS at the Fermi energy was too large. In accord with Sticht and Kübler he assigns a significant part of the DOS to minority 4f states. However, he concludes that the band model is more appropriate for Gd, because he found Fermi surface sections in agreement with de Haas–van Alphen experiments [16, 17] that depend on the hybridization of the 4f bands with other valence bands. This conclusion was contradicted by Ahuja *et al* [18], who stated that they believe that one does not need to explicitly include the d–f hybridization in the calculation in order to describe the small orbits of the Fermi surface.

The first total-energy full-potential linearized augmented plane-wave (FLAPW) calculation of the magnetic ordering at the Gd(0001) surface [19] using the 4f-core model reported an antiferromagnetic (AFM) coupling of the surface layer with respect to the bulk, in agreement with an early interpretation of experimental data [20]. This result stimulated a number of theoretical studies by several authors, investigating the magnetic coupling of Gd, both at the (0001) surface and in the bulk. Heinemann and Temmerman [21, 22] were the first to show that the 4f-band model in LDA predicts not only an AFM coupling between the first

and second surface layers, but also a layerwise AFM order in hcp bulk Gd. On the contrary, the ground state was found to be FM, applying the generalized gradient approximation (GGA). Using the linear muffin-tin orbital (LMTO) method in the atomic sphere approximation (ASA), Bylander and Kleinman published a series of studies [8–10], concentrating on the adequacy of LDA for the Gd 4f states. By comparing Hartree–Fock with atomic LDA calculations [8] they concluded that the minority 4f resonance in the metal right above E_F, which is responsible for the enhanced DOS $N(E_F)$, is an artifact of the LDA. In a second paper the authors suggested a new approach, treating the majority 4f states as localized and fully occupied and the minority states in the band Hamiltonian. The effective potential in the latter calculations was constructed from Hartree–Fock theory for the core density and from LDA for the valence charge density. A single parameter was used to fit the calculated bulk magnetic moment to the experimental value. This constraint on the calculation has the effect of pushing the minority 4f states to higher energies. In fact, the authors found the minority 4f states at a much higher energy (8.4 eV above E_F) than an inverse photoemission experiment (IPE) [23] (4.3 eV). With this model they found a much smaller value of $N(E_F)$ and also an equilibrium lattice constant in good agreement with experiment. Bylander and Kleinman [9] also performed total-energy calculations for the AFM bulk phase. However, they found the correct FM ground state. They extended their study to the Gd(0001) surface [10], using the same model as in the previous publication. In contrast to a former study by Wu *et al* [19], which predicted an outward relaxation by 6.3% for the FM surface, they found a contraction by 3.4% in agreement with a low-energy electron-diffraction (LEED) experiment [24]. Comparing FM and AFM coupling of the first layer to the bulk, they discovered a lower total energy for the FM configuration, which also contradicted the results of [19]. Eriksson *et al* [25] investigated the magnetic coupling for hcp bulk Gd and the Gd(0001) surface. They applied the full-potential linear muffin-tin orbital (FP-LMTO) method. Applying the 4f-band model to bulk Gd they found an AFM ground state, irrespective of whether they used LDA or GGA. However, the application of the 4f-core model led to the prediction of the correct FM ground state. Consequently, Eriksson *et al* adopted this approach for their surface calculation, also finding an FM coupling of the surface layer to the bulk and an inwards relaxation of 4.4%, in reasonable agreement with the results of Bylander and Kleinman [10]. A different approach has been used by Shick *et al* [11, 12]. They apply the so-called LDA + U energy functional [26] for the description of the localized 4f electrons. Within this model the strong intra-atomic interactions of the localized states are introduced and treated in a Hartree–Fock-like manner. One effect of this model is that the occupied and unoccupied 4f states split apart. The minority 4f states are shifted away from the Fermi energy to higher energies, removing the artifact from the LDA. At the same time the majority 4f states are shifted to lower energies. In contrast to the 4f-core model, using the LDA + U description the majority 4f states still hybridize slightly with the states of the neighbouring atoms and the 4f majority charge density is slightly more contracted. They found the correct FM ground state for hcp Gd and also an FM coupling of the surface layer of Gd(0001). In addition, they reported that surface relaxation led of to a 90% enhancement of the effective exchange coupling of the FM surface layer to the adjacent bulk layers, resulting in a 30% increase of the surface Curie temperature, in agreement with several photoemission and photoelectron diffraction experiments [27–30].

In this paper we want to show that removal of the minority 4f states from the Fermi energy—irrespective of the particular model—leads to a correct description of the magnetic ordering both for the bulk and the surface, while other quantities, such as lattice constants or magnetic moments, depend sensitively on the exact energetic position of the 4f states and, therefore, on the model used. After a short presentation of the calculational method, we first turn to bulk hcp Gd and apply the 4f-band and 4f-core models in LDA and GGA. We also

present results of a 'hybrid' approach as well as LDA + U results. Then we focus on the (0001) surface of Gd and conclude with the investigation of the surface states observed in scanning tunnelling spectroscopy experiments.

2. Computational details

We use the FLAPW method [31, 32] for bulk and film calculations as realized in the FLEUR code. Calculations in the LDA applied the parametrization according to Moruzzi *et al* [33] and those in the GGA the parameters of Perdew and Wang [34]. During the calculation of the equilibrium lattice constant, the c/a ratio was kept fixed at the experimental value of 1.597 [35]. The plane-wave cut-off for the basis functions was set to $K_{\max} = 3.0\ \text{au}^{-1}$. This corresponds to about 100 basis functions per atom. The charge density and the potential were expanded up to a cut-off $G_{\max} = 9.0\ \text{au}^{-1}$. We set the muffin-tin radii to $R_{MT} = 2.80$ au. The wavefunctions as well as the density and the potential were expanded up to $l_{\max} = 8$ inside the muffin-tin spheres. The 5s and 5p semi-core states were treated as valence states in a separate energy window. (The influence of the treatment of the 5p states in Gd was discussed by Temmerman and Sterne [36].) For the bulk calculations we used $\boldsymbol{k}$-point sets that correspond to 320 and 1152 $\boldsymbol{k}$-points in the full Brillouin zone in the semi-core and the valence window, respectively. The surface calculations were performed using a symmetric ten-layer Gd film embedded in semi-infinite vacua. All cut-off parameters were chosen as for the bulk calculations. The integrations over the two-dimensional Brillouin zone were carried out using $\boldsymbol{k}_{\parallel}$-point sets that correspond to 81 and 361 $\boldsymbol{k}_{\parallel}$-points in the full two-dimensional Brillouin zone for the semi-core and the valence window, respectively. The implementation of the LDA + U [26] formalism is similar to Shick *et al* [11] but without the pseudoperturbative treatment described in this reference. We used the same parameters as in [11], i.e. $U = 6.7$ eV and $J = 0.7$ eV, but, if not stated otherwise, we used also for the LDA + U calculations $R_{MT} = 2.80$ au. In these calculations the semi-core states were treated using local orbitals [37].

3. Bulk hcp Gd

In this section we investigate the effect of different models to treat the 4f states on the ground-state properties of bulk Gd. Although numerous studies of this system can be found in the literature, they do not allow a direct comparison since they were derived with different computational methods (pseudopotentials, LMTO, LAPW, ASW etc). Here, we compare the application of LDA as well as GGA potentials and the 4f-band and the 4f-core as well as a 'hybrid' approach and the LDA + U model within the same (FLAPW) framework.

3.1. Band structure and density of states

In figure 1 we present results of an LDA calculation in the 4f-band model, where the 4f electrons are treated as valence electrons on the same footing as the 6s and 5d states. The band structure was calculated at the experimental lattice constant of 6.858 au. The most prominent feature is the nearly dispersionless majority 4f bands about 4.5 eV below the Fermi energy (left-hand panel) and the minority 4f bands directly above the Fermi energy (right-hand panel). The result is in good agreement with previous first-principles calculations that used the 4f-band model (see e.g. [7, 15]). However, these studies used fully relativistic methods, while we applied the scalar relativistic approximation, which neglects the spin–orbit coupling. The spin–orbit coupling leads to a splitting of the 4f bands broadening the majority and minority 4f bands to a width of 0.7 eV. Therefore, the bandwidth of the 4f band we found, in particular the majority

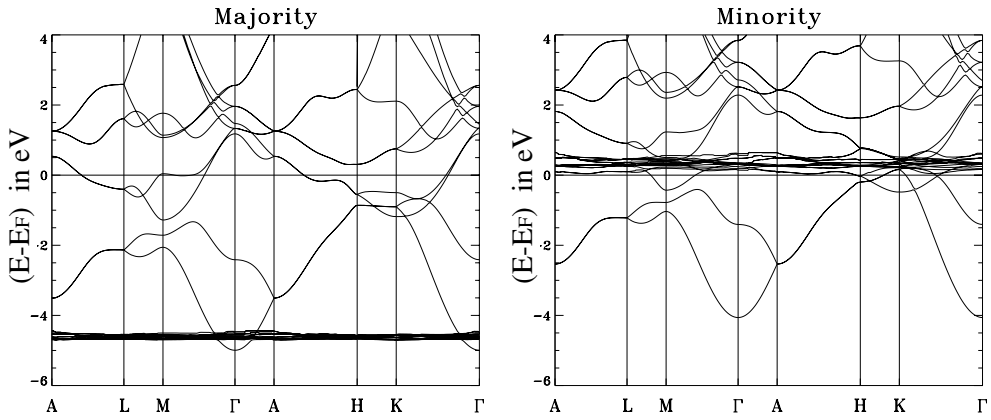

Figure 1. LDA band structure of hcp bulk Gd, calculated within the 4f-band model. The majority spin states are shown in the left-hand panel and the minority states in the right-hand panel.

Table 1. Magnetic moment and 4f charge calculated at the experimental lattice constant (3.629 Å) with different models. The first three columns contain the magnetic moment in the muffin-tin sphere and the valence- and d-electron contribution to it. The fourth column contains the total magnetic moment per atom, including the interstitial contribution. All moments are in units of μ_B. The last two columns contain the majority and minority 4f charge in units of electrons.

Model		M (μ_B)	val. (μ_B)	d (μ_B)	tot. (μ_B)	f ↑ (e^-)	f ↓ (e^-)
	4f band	7.21	7.21	0.34	7.63	6.94	0.13
LDA	4f core	7.41	0.41	0.36	7.80	—	—
	$+U$	7.41	7.41	0.39	7.82	6.95	0.01
GGA	4f band	7.22	7.22	0.34	7.65	6.65	0.12
	4f core	7.41	0.41	0.35	7.81	—	—

part, is smaller than in these previous studies. Experimentally the majority and minority 4f bands are found at about 8 eV below and 4.5 eV above the Fermi energy, respectively. Thus, the wrong energetic positions of the 4f bands are artifacts of the LDA. The LDA overestimates the itinerancy of the 4f electrons. The minority 4f state, located just above E_F, leads to an additional DOS at E_F. Close to the Fermi energy the 4f states hybridize with the d states in that energy region. In fact, we found about 0.12 minority electrons with f character inside the muffin-tin spheres (cf table 1). Hence, parts of the minority 4f, or the f–d-hybridized, bands are occupied, which is unphysical, and has direct consequences for the magnetic order, as we shall discuss below. Another band that has been observed by photoemission is the spin-split Δ_2 band, which is the second lowest occupied minority band at the Γ-point and its majority counterpart. The calculation shows that it has mainly d, but also considerable s character. At the Γ-point we found the majority state $\Delta_{2\uparrow}$ at 2.4 eV and the minority state $\Delta_{2\downarrow}$ at 1.4 eV below the Fermi energy, in agreement with earlier calculations [7,15]. Experimentally the $\Delta_{2\uparrow}$ and $\Delta_{2\downarrow}$ bands are found 2.4 eV and 1.7 eV below E_F, respectively [38].

The difference between the results obtained in the LDA and GGA is marginal when the calculations are performed at the experimental lattice constant. The majority 4f bands are found about 0.2 eV lower than in the LDA calculation; the changes of the other bands are even smaller. Therefore, we shall not present the GGA band structure.

Next we present the result of an LDA calculation with the 4f-core model, also for the experimental lattice constant. Within this method, the majority 4f electrons are treated as core

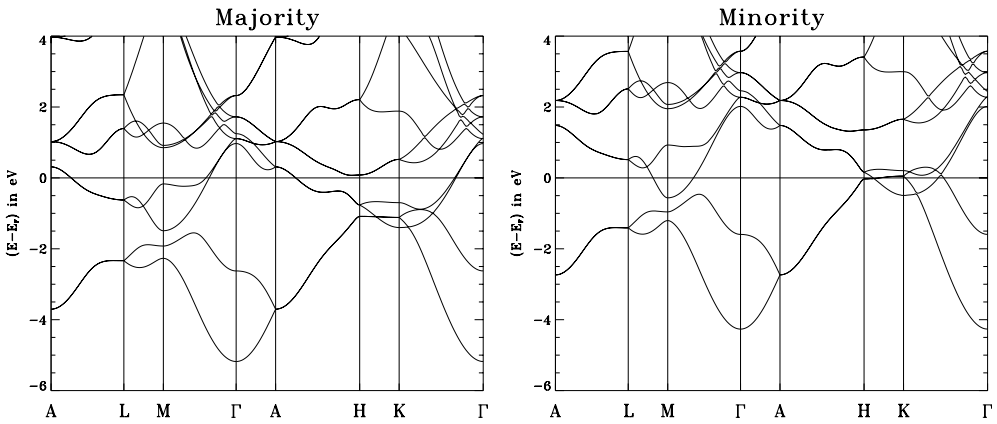

Figure 2. LDA band structure of hcp bulk Gd, calculated within the 4f-core model. The majority spin states are shown in the left-hand panel and the minority states in the right-hand panel.

electrons, i.e. they are not allowed to hybridize with any other states on neighbouring atoms. Thus, the bonding of the 4f electrons is neglected. Technically speaking, within the FLAPW method this means that we have to prevent the majority and minority 4f bands from appearing in the valence-band energy window for which we determine the eigenvalue spectrum. This is done by moving the minority and majority 4f energy parameters to a value far above the Fermi energy. In all 4f-core calculations presented here, the valence majority and minority f energy parameters have been set to about 9.5 eV above E_F. Thus, we have practically removed the f functions from the basis set. The calculated band structure is shown in figure 2. The 4f states are no longer in the valence band structure. If the core electrons were included in the band structure plot, the majority 4f electrons would appear at almost the same energy as in figure 1 but as a dispersionless straight line. Another difference to the result of the 4f-band calculation is that the Fermi energy is shifted upwards by about 0.2 eV with respect to the minimum of the valence band. In the 4f-band model the Fermi energy was pushed down by the large DOS of the minority 4f states. Due to the change of E_F, the $\Delta_{2\uparrow}$ band is now found at 2.6 eV below E_F at the Γ-point and the $\Delta_{2\downarrow}$ is found at 1.6 eV below E_F. Apart from this shift the band structure of the valence bands is largely unchanged. Only the minority d bands that are in the region of the 4f states right above the Fermi energy in the 4f-band calculation differ from those of the 4f-core calculation. However, the difference is typically $<$0.2 eV. This is probably a consequence of the unphysical hybridization with the 4f states. As in the 4f-band calculation the GGA results are very similar to the LDA results and therefore the GGA band structure is not shown here.

To illustrate the effect of the inclusion of a Hubbard U in the density functional, we plot the DOS of FM hcp Gd as calculated with the LDA and the LDA+U model in figure 3. In LDA the splitting between the majority and minority 4f states is only about 5 eV, while LDA + U increases this splitting close to the experimentally observed value of 11 eV [11]. The most important effect, however, is that the minority 4f band is now pushed 2 eV upwards and there are virtually no occupied minority 4f electrons left. This is responsible for the change in the magnetic coupling of the Gd atoms: in LDA + U the magnetic ground state of hcp Gd is FM. The other changes in the DOS are small: the majority (s, d) band is found 0.3 eV lower than in LDA, but unchanged otherwise. The occupied part of the minority (s, d) band is almost unchanged.

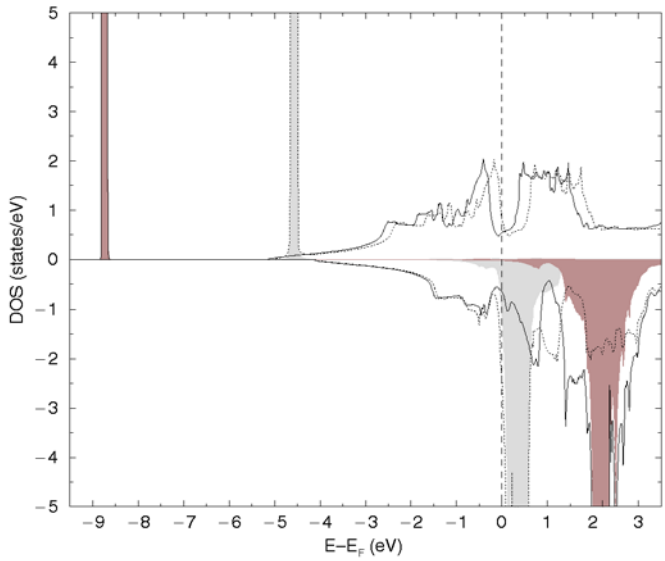

Figure 3. DOS of FM hcp Gd calculated with the LDA (dotted curves) and the LDA + U (full curves) model. The dark (light) shaded areas indicate the position of the 4f band in LDA + U (LDA). Minority states are plotted with negative values of the DOS.

3.2. Magnetic properties

Table 1 gives an overview over the calculated magnetic moments and the 4f charge obtained with the different models. The total magnetic moment per atom is given in the fourth column. All other quantities are integrated over the muffin-tin spheres. In the FLAPW method the muffin-tin spheres do not cover the whole volume of the unit cell, i.e. the contribution from the interstitial region adds to these quantities. The size of this difference can be appreciated from a comparison of the first column, which contains the magnetic moment in the muffin-tin spheres, and column four, which contains the total moment per atom. Comparing the results of the 4f-band model, the total moment per atom is in excellent agreement with other recent results (e.g. [11, 40]) and also with the experimental value of 7.63 μ_B. However, the 4f-core model yields a slightly larger value, which has already been observed by other authors (e.g. [25]). The moment of the 4f-core calculation is in nearly perfect agreement with our LDA + U calculation and the values of Shick *et al* [11]. A small increase of the d moment (due to the shift of the majority (s, d) band visible in figure 3) results in a slightly higher total magnetic moment, but irrespective of the model used, the d moment in the muffin-tins is always $\approx$0.35 μ_B. The total moment in the muffin-tin sphere using the 4f-band model is 7.21 μ_B. This is smaller than one would expect from the 7 μ_B of the 4f electrons and the polarization of the s and p electrons. In the 4f-core model the valence moment in the sphere amounts to 0.41 μ_B (here the 4f electrons are excluded from the valence), i.e. the total valence moment is larger than the d moment due to the contribution of the s and p electrons. The difference between the 4f-band and the 4f-core results is mainly due to the occupation of the minority 4f band in the 4f-band model, which reduces the total 4f moment. The majority 4f states are always fully occupied. However, the majority 4f charge in the muffin-tins is slightly smaller than 7 e^-, because the majority 4f states are not completely localized inside the muffin-tin sphere in either LDA or GGA. In general it can be said that the differences between LDA and GGA are marginal, irrespective of whether the 4f-band or the 4f-core model is used. The only difference that might be important is that

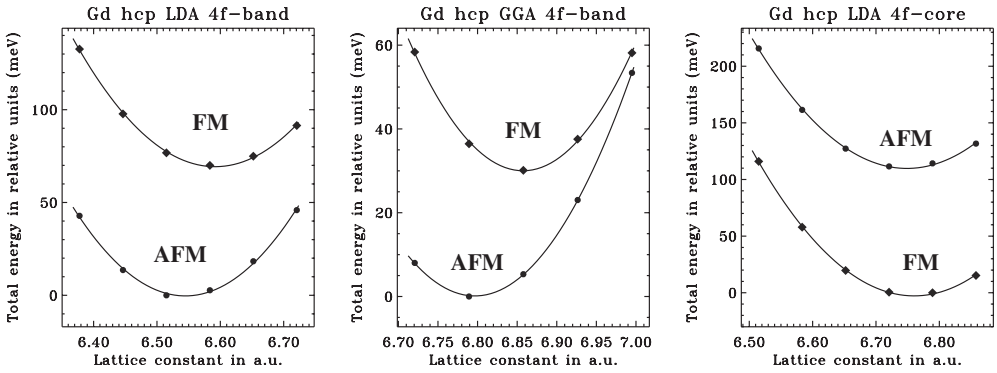

Figure 4. Energy as a function of the lattice constant for hcp bulk Gd in the FM (diamonds) and AFM (circles) states. The solid lines are parabolic fits that have been used to determine the equilibrium lattice constant. The left and the centre panels show the results of LDA and GGA calculations, respectively. In both cases the 4f-band model has been applied. The right-hand panel contains the result of an LDA calculation within the 4f-core model.

the unphysical minority 4f occupation in the 4f-band model is slightly reduced when the GGA is applied.

3.3. Equilibrium lattice constant and magnetic structure

In the next step we investigated the magnetic ground state of hcp Gd. We performed total-energy calculations to determine the equilibrium lattice constant for the FM and AFM configurations. The AFM configuration consists of AFM layers in the (0001) direction, i.e. the magnetic moments of the two atoms of the hcp unit cell are aligned anti-parallel. The total energy as a function of the lattice constant obtained using the LDA 4f-band model, the GGA 4f-band method and the LDA 4f-core model is presented in figure 4. The 4f-band model calculations predict an AFM ground state, irrespective of whether the LDA or the GGA functional is applied. This result is in agreement with previous full-potential calculations [11, 25]. However, it was reported [21, 40] that using the GGA 4f-band model in combination with the LMTO method in the ASA yields the correct FM ground state. We speculate that this is an effect of the ASA in combination with GGA [41, 42]. The picture changes when the 4f-core model is used (right-hand panel). The LDA 4f-core model predicts the FM ground state. This is also true for the GGA 4f-core model, which is not shown in figure 4.

All calculations that use the 4f-band model agree in that they find the minority 4f states very close to the Fermi energy. This leads to densities of states at the Fermi energy which are too large compared with experiment and leads to an unphysical partial occupation of the 4f states. In figure 5 we observe that for the AFM state the minority 4f band is narrower and shifted to higher energies as compared with the FM state. The AFM coupling reduces the covalent repulsion and this might lead to a stabilization of the AFM state. A similar effect is observed when we increase the lattice constant of Gd: this affects both the FM and the AFM states and leads—at larger volumes—to a reduction of the energy difference between these magnetic configurations. This effect can be seen in figure 4 for the LDA and GGA 4f-band model whereas the energy difference increases with increasing lattice constant in the calculation within the 4f-core model. Due to the 4f minority states close to the Fermi energy, we also expect a direct 4f–4f hybridization with a strong AFM susceptibility, similar to the case of d–d hybridization [43].

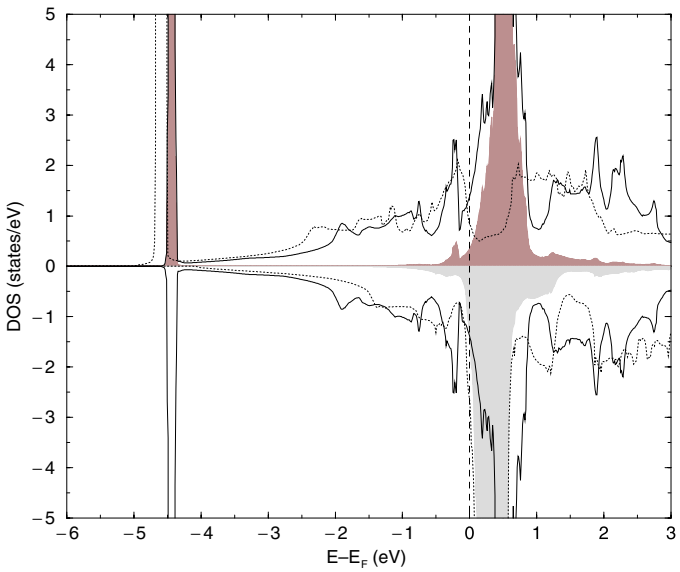

Figure 5. DOS of FM (dotted curves) and AFM (full curves) hcp Gd calculated within the LDA. The light (dark) shaded areas indicate the position of the 4f band in the minority (majority) channel of the (A)FM DOS. Minority states are plotted with negative values of the DOS.

We can quantify the contribution of the s, p, d and f states to the energy difference between the FM and the AFM states in the 4f-band model by applying the magnetic force theorem in the frozen potential approximation. We start from a self-consistent potential but set the exchange–correlation B-field in the interstitial to zero and make two nonself-consistent calculations whereby in one case the B-field in the muffin-tin of every second close-packed plane of atoms is sign reversed. Then, the difference of the eigenvalue sums of these two calculations approximates the total-energy difference of the FM and the AFM state. By weighting the eigenvalues with their l-like local partial charges we can calculate the contributions of the different l-channels to this energy difference. For this calculation we used the theoretically determined lattice constant and a large muffin-tin radius of 3.2 au. We started from the potentials of both a ferro- and an antiferromagnetic calculation and obtained similar results. Here we quote the averaged values. This analysis shows that the p- and d-like states clearly favour an FM coupling (76 meV/atom) while the f states strongly prefer an AFM order (-128 meV/atom). Most of this energy originates from the minority 4f band. The s electrons make only a small FM contribution that, in total, leads to a stabilization of the AFM states by -38 meV/atom.

These observations suggest that the incorrect description of the 4f minority states in the LDA (and GGA) is the reason for the prediction of the wrong magnetic ground state. In fact, models that have the effect of pushing the 4f states away from the Fermi energy, such as the Hartree–Fock treatment of the exchange between the core and the valence electrons [9] or the LDA + U model [11], or models that do not allow for 4f electrons in the valence band region, such as the 4f-core model [25], found the correct ground state. To substantiate the argument on the role of the minority 4f states presented above, we performed a further calculation using a 'hybrid' approach, where we treat the majority 4f electrons as valence electrons, but remove the minority 4f electrons from the valence-band region by shifting the minority f energy parameter far above the Fermi energy as in the 4f-core calculation. In fact, this calculation predicts the FM ground state. The total energy difference between the FM and AFM states is very close

Table 2. Equilibrium lattice constants (relative to the experimental value of $a_{0,\mathrm{exp}} = 3.629$ Å [35]), magnetic moments in the muffin-tin spheres at these lattice constants and the energy difference between the AFM and FM states at the respective equilibrium lattice constants for hcp bulk Gd, calculated using different models to treat the 4f states. Positive (negative) energy differences refer to an FM (AFM) ground state. In the last column a simple estimate of the Curie (Néel) temperature from the nearest-neighbour Heisenberg model is given. (Note that this table contains data at the calculated equilibrium lattice constants and the muffin-tin radii used are smaller that that used in [12].)

Model		$\Delta a_{0,\mathrm{FM}}$ (%)	M_{FM} (μ_B)	$\Delta a_{0,\mathrm{AFM}}$ (%)	M_{AFM} (μ_B)	$E_{\mathrm{AFM}} - E_{\mathrm{FM}}$ (meV atom^{-1})	$T_{C(N)}$ (K)
LDA	4f band	−3.9	7.15	−4.6	7.10	−69	534
	4f core	−1.4	7.41	−1.7	7.32	56	433
	hybrid	−2.7	7.38	−2.8	7.29	60	464
	$+U$	−2.7	7.39	−3.4	7.31	34	263
GGA	4f band	−0.0	7.22	−0.9	7.13	−15	116
	4f core	+1.6	7.41	+1.5	7.34	55	425

to that calculated with the 4f-core model (cf table 2). Finally, we also applied the LDA + U model to the problem. The 4f minority band is now only 2 eV above the Fermi level, but this is still enough to stabilize the FM solution by 34 meV.

Table 2 summarizes the calculated lattice constants, the magnetic moments at the equilibrium lattice constant and the energy difference between the FM and the AFM configuration. As we have already pointed out, the 4f-band model predicts the incorrect magnetic ground state. In contrast, the 4f-core model and also the hybrid approach, which treats the majority 4f electrons as band electrons but removes the minority 4f electrons from the vicinity of the Fermi energy, yield the FM ground state. Apparently, the half-filled 4f band that crosses the Fermi energy is the reason for the AFM coupling, in analogy with half-filled 3d bands that have a strongly AFM susceptibility. Thus, it is the unphysical partial occupation of the minority 4f bands that causes the incorrect description of the magnetic ground state of Gd in the LDA/GGA 4f-band model. The LDA/GGA 4f-core model and the hybrid approach predict almost the same energy difference of about 55 and 60 meV/atom, respectively, between the FM and AFM states. These energy differences are also in reasonable agreement with other models that remove the minority 4f states from the region close to the Fermi energy (Hartree–Fock valence–core exchange, 118 meV/atom [9]; LDA 4f core, ≈ -0.08 eV; GGA 4f core, ≈ -0.10 eV [25]; LDA + U, 63 meV/atom [11]).

It might be of interest to mention here that the difference between our LDA+U result and the results of Shick *et al* is only partially due to the fact that in [11] the experimental lattice constant was used. In this reference the muffin-tin radii were 3.2 au, while we used 2.8 au. While other quantities (e.g. the DOS, magnetic moments etc) are rather insensitive to the choice of the muffin-tin radius, in Gd the total-energy difference between the FM and the AFM state depends very sensitively on this parameter. A calculation assuming the theoretically determined equilibrium lattice constants with a muffin-tin radius of 3.2 au yields an energy difference of 51 meV, i.e. 50% larger than in the calculation with the smaller radii. This large difference might result from the extreme sensitivity of the energy to the (although very small) number of occupied minority 4f electrons and might therefore be a unique feature of metallic Gd. Due to the higher degree of localization of the 4f-states in AFM Gd, in this magnetic configuration the number of occupied minority 4f electrons is about 0.01 larger than in the FM configuration.

In table 2 we also listed the Curie (Néel) temperatures of bulk Gd as calculated from the total energy difference of the FM and the AFM state in the nearest-neighbour Heisenberg

model [12]. Here, we start with the conventional Heisenberg Hamiltonian

$$\mathcal{H} = -J \sum_{i,j} \vec{S}_i \vec{S}_j, \tag{1}$$

which describes the isotropic exchange interaction, J, between the spins located in the three-dimensional lattice. We assume that the exchange interaction between nearest-neighbour atoms is the dominant one (although to our knowledge this has not been proven so far, nor is it trivial, as the RKKY interaction of itinerant d electrons mediating the interaction is long range and falls off slowly), thus the summation runs over all nearest-neighbour sites. For the moment we assume an ideal c/a ratio of $\sqrt{8/3} \approx 1.633$, so that each atom has 12 nearest neighbours. Then, the transition temperature of the conventional isotropic three-dimensional Heisenberg ferromagnet in the mean-field approximation is given by

$$T_C^{\mathrm{MF}} = 12\, J\, \frac{S(S+1)}{3k_B} = 2\frac{E_{\mathrm{AFM}} - E_{\mathrm{FM}}}{3k_B}. \tag{2}$$

Compared with the experimentally determined Curie temperature of 293 K, most models tend to overestimate T_C (cf table 2; we used the energy difference at the respective equilibrium lattice constant and the experimental c/a ratio). The fact that our value obtained with the LDA + U model is 10% too small is an effect of the chosen size of the muffin-tin radius rather than of the model itself. As discussed above, with a larger radius a larger value of $E_{\mathrm{AFM}} - E_{\mathrm{FM}}$ is obtained, leading to a calculated Curie temperature of 395 K.

A better approximation to T_C was suggested by Rushbrook and Wood [44], who derived for a face-centred cubic (fcc) lattice the approximate expression

$$T_C = \frac{25}{96}\frac{J}{k_B}[11S(S+1) - 1]. \tag{3}$$

In the nearest-neigbour approximation for the ideal c/a ratio the hcp and the fcc lattice are equivalent. Applying this expression, T_C is reduced by roughly 28%, which results, for the 4f-core model, in a Curie temperature of 311 K, which is already remarkably close to the experimental value.

Due to the deviation from the ideal c/a ratio the interatomic exchange constants in the close-packed (0001) planes, $J_\parallel$, and between these planes, $J_\perp$, are slightly different. From our calculations we can only access $J_\perp$ directly. As we have already shown, in the 4f-band model, increasing the Gd lattice constant results in a reduction of the energy difference between the AFM and the FM state. It was also shown by Jenkins and Temmerman [45] that increasing the c/a ratio from the experimental value of 1.58 to the ideal one of 1.63 lowers this energy difference by approximately 5 meV, in both the LDA and GGA. From this we can speculate that the in-plane $J_\parallel$ is about 10% smaller than the $J_\perp$ coupling the close-packed (0001) planes and our estimation for T_N might be 5% too high. In the 4f-core model $E_{\mathrm{AFM}} - E_{\mathrm{FM}}$ increases slightly, thus the estimates for T_C will be a little too low.

In addition to the incorrect description of the magnetic coupling, the LDA 4f-band model yields a lattice constant that is 3.9% too small, which is more than the average LDA error. This is a result of the fact that the LDA overestimates the itinerancy of the 4f states and thus the 4f bonding. With the hybrid approach this error becomes smaller. The 4f-core model yields a value which is only 1.4% smaller than experiment. However, in the latter model all 4f bonding is neglected. In the LDA + U calculation a larger relaxation similar to the hybrid approach is found. The lattice constant calculated using the GGA 4f-core model is 1.5% too large. A similar deficiency of the GGA was found for the 4d and 5d transition metals [46].

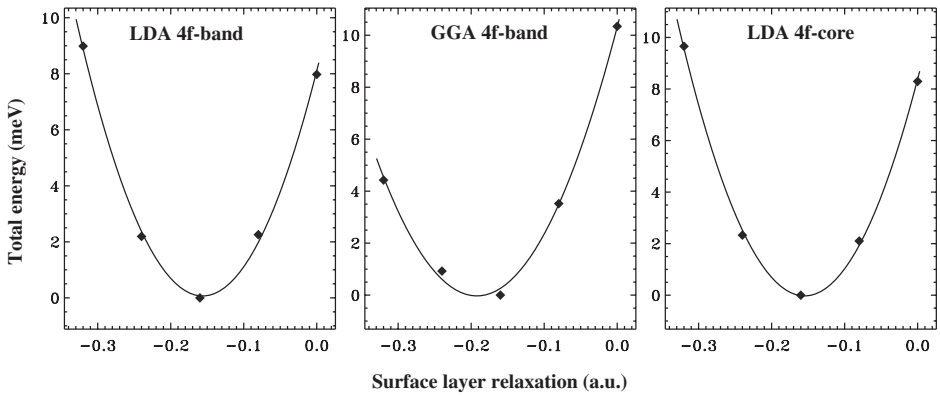

Figure 6. Energy in meV as a function of the interlayer distance in au between the surface and subsurface layer of the FM Gd(0001) surface. The solid curves are parabolic fits that have been used to determine the equilibrium interlayer distance. The zeros of the energy scales were chosen at the equilibrium configuration. The left and the centre panels show the results of LDA and GGA calculations, respectively. In both cases the 4f-band model has been applied. The right-hand panel contains the result of an LDA calculation within the 4f-core model.

4. Gd(0001) surface

4.1. Relaxation

We focus first on the determination of the atomic structure of the FM Gd(0001) surface. Using self-consistent total-energy calculations we determined the relaxation of the surface layer, applying three different models, the LDA/GGA 4f-band model and the LDA 4f-core model. We started from the equilibrium bulk atomic positions of the respective bulk calculation, i.e. the LDA/GGA 4f-band result and the LDA 4f-core result. We then varied the interlayer spacing between the surface and the subsurface layer to find the equilibrium position of the surface layer. Figure 6 shows the total energy per surface atom as a function of the interlayer distance. In all models to treat the 4f bands we found a contraction of the interlayer spacing between the surface and the subsurface layer, d_{12}. With the GGA 4f-band model we obtain an inwards relaxation, Δd_{12}, of 3.5% of the bulk interlayer distance, and with the LDA 4f-band/4f-core model we obtain a 3.0 and 2.9% relaxation, respectively. These results are in good agreement with the experimental LEED result of Quinn *et al* [24] of $\Delta d_{12} = 3.5 \pm 1.0\%$ for bulk Gd (0001) surfaces and Giergiel *et al* [39], who obtained $\Delta d_{12} = -2.4\%$ for thick epitaxial Gd (0001) films on W(110) (in this work an expansion of the interlayer spacing between the sub- and the subsubsurface layer $\Delta d_{23} = 1.0\%$ was reported). Recent first-principles calculations found relaxations Δd_{12} of 4.4% [25] and 3.4% [10]. Table 3 summarizes the relaxation and the magnetic moments of all atoms in the ten-layer film.

4.2. Magnetism

The magnetic moments have been calculated for the surface atom in the relaxed position. However, the moment does not depend critically on the relaxation. In fact, we found exactly the same moment of the surface atom for the ideal bulk truncated position, e.g. for the LDA 4f-core calculation. A major difference between the 4f-band calculations and the 4f-core calculation is found for the magnetic moment of the surface atom. While the 4f-band model does not show an indication of an enhanced surface moment, the 4f-core model predicts a surface moment

Table 3. Relaxation of the surface layer of the Gd(0001) surface and the magnetic moments of the different layers (S = surface, $S-1$ = subsurface, ...). Δd_{12} is the relative change of the distance between the surface and the subsurface layer with respect to the respective bulk value.

Model		Δd_{12} (%)	M_S	M_{S-1}	M_{S-2} (μ_B)	M_{S-3}	M_{S-4}
LDA	4f band	−3.0	7.21	7.19	7.20	7.18	7.20
	4f core	−2.9	7.55	7.41	7.40	7.42	7.41
GGA	4f band	−3.5	7.20	7.21	7.22	7.22	7.24

Table 4. Energy difference (in meV per surface atom) between the FM and AFM coupling of the surface layer to the underlying bulk layers of the Gd(0001) surface. The energies were calculated with the surface atom in the ideal truncated bulk position (unrelaxed) and in the relaxed position using the 4f-band, the 4f-core and the hybrid and the LDA + U model. Positive energy differences refer to an FM coupling.

		$E_{\mathrm{AFM}} - E_{\mathrm{FM}}$ (meV/surface atom)	
Model		Unrelaxed	Relaxed
LDA	4f band	25	20
	4f core	100	108
	hybrid	99	106
	+U	89	95

enhancement of about 0.15 μ_B, in good agreement with previous calculations [12, 25]. We attribute this enhancement of the surface moment to the increase of the d moment due to the d-band narrowing as result of the reduced number of nearest neighbours at the surface. In the 4f-band calculation this enhancement of the d moment is cancelled by an increased occupation of the minority 4f bands.

In addition to the FM surface we also performed calculations for an FM surface layer coupling antiferromagnetically to the underlying bulk using the LDA 4f-band, 4f-core, the hybrid and the LDA + U models. These calculations were carried out with the surface atom in the respective ideal bulk truncated positions as well as in the equilibrium positions of the FM surfaces. (For the hybrid and the LDA + U calculations the relaxations were taken from the LDA 4f-core calculation.) In all cases we found that the system with a ferromagnetically coupled surface layer is the magnetic ground state of the Gd(0001) surface. In contrast to [19], we found even for calculations within the 4f-band model the lowest energy for FM coupling. However, the energy differences between the FM and the AFM configuration vary among the models: in the LDA 4f-band model we find an energy difference of just 25 meV. As soon as the 4f minority states are removed from the Fermi energy as in the 4f-core, the hybrid or the LDA + U model, the energy difference increases to about 100 meV. This is in good agreement with the result of Eriksson *et al* [25], who found about 95 meV per surface atom in the 4f-core model. Thus, the surface results confirm the result of the bulk calculations, i.e. that the minority 4f states right above the Fermi energy act in favour of AFM coupling.

Surface relaxation increases the energy difference between the FM and the AFM state by about 7 meV per surface atom with the exception of the LDA 4f-band calculations, where the energy is reduced by about the same amount. For example, in the 4f-core model the energy difference increases from 100 meV per surface atom to 108 meV (cf table 4). This small enhancement of the FM coupling is also supported by the work of Jenkins *et al*, who found a clear dependence of the magnetic coupling on the c/a ratio for the Gd(0001) surface [45] and hcp bulk Gd [40] using the GGA 4f-band model. However, Shick *et al* [12], using the LDA + U

model found even larger energy differences between the unrelaxed and the relaxed surfaces. Using a seven-layer slab with the experimental lattice constant they found for the ideal bulk truncated surface a relatively small value of the energy difference (72 meV per surface atom) that, assuming the experimentally observed relaxation [39], increased to 135 meV. Based on this large energy increase between FM and AFM coupling in the relaxed position of the surface layer, they argued that the increased magnetic coupling strength between the surface and the subsurface layer is the origin of the enhanced surface Curie temperature that has been observed in many experiments [30]. Our calculations, however, predict even for the unrelaxed surface an enhancement of the Curie temperature at the surface. Applying the model put forward in [12], in the 4f-core model a ratio of surface-to-bulk T_C of 1.14 is obtained. In agreement with [12], the magnetic coupling is larger for the relaxed surface than for the unrelaxed one, leading to a further enhancement of the surface Curie temperature. In the 4f-core model at the relaxed surface T_C is enhanced by 21%; experimentally 29% was found [30]. From our bulk calculations we have seen that in the LDA+U model the energetics can depend on the size of the muffin-tin radius, therefore our results allow no direct comparison to [12]. Furthermore, other computational details such as the different number of layers in the film, different relaxations and lattice constants might account for the observed differences in the calculations. Therefore, the physical origin of the large magnetoelastic effects observed in [12] still has to be explained. Also experimentally the question of whether there is an increase of the Curie temperature at the Gd(0001) surface seems not to be finally resolved since new measurements report no extraordinary transition at the surface [47].

4.3. Band structure

After the determination of the ground-state structure we turn to the electronic structure of the FM Gd(0001) surface. As in the case of hcp bulk Gd we present the band structure determined within the LDA 4f-band model (figure 7) and the LDA 4f-core model (figure 8), both calculated in the respective equilibrium structure. In the 4f-band model, as in the bulk band structure (figure 1), the nearly dispersionless 4f bands are 4.4 eV below the Fermi level (majority states, left-hand panel of figure 7) and 0.5 eV above E_F (minority states, right-hand panel of figure 7). The most interesting feature of the band structure is the surface state that is found in a gap of the projected bulk band structure around the $\overline{\Gamma}$-point. The surface state with majority spin character (left-hand panel of figure 7) is occupied and found 0.15 eV below the Fermi energy. This surface state has been investigated experimentally by various techniques, including photoemission [29] and scanning tunnelling spectroscopy (STS) [48], and is found around 0.20–0.25 eV below the Fermi energy. The surface state with minority spin character can be seen in the right-hand panel of figure 7. It is unoccupied and lies directly above the minority 4f bands at the $\overline{\Gamma}$-point at 1.04 eV above the Fermi energy. Experimentally [48] it is found at about 0.40–0.50 eV. Thus, the theoretically determined exchange splitting of the surface state is 1.2 eV, while experimentally a smaller value of $\approx$0.7 eV is found. Both the minority and the majority part of the surface state are strongly localized at the surface. Our calculations show that over 70% of their charge density is found in the surface layer and the vacuum region. An analysis of the charge density of the surface state in the muffin-tin spheres at the surface atoms shows that is has mainly 5d character. Our band structure is in excellent agreement with the results of Wu *et al* [19], who also found the minority part of the surface state more than 1 eV above the Fermi energy. However, they used a six-layer Gd film. As a consequence, a splitting of the surface state due to the finite size of the film is clearly visible in their calculation. With a ten-layer film such a splitting is no longer visible in the vicinity of the $\overline{\Gamma}$-point.

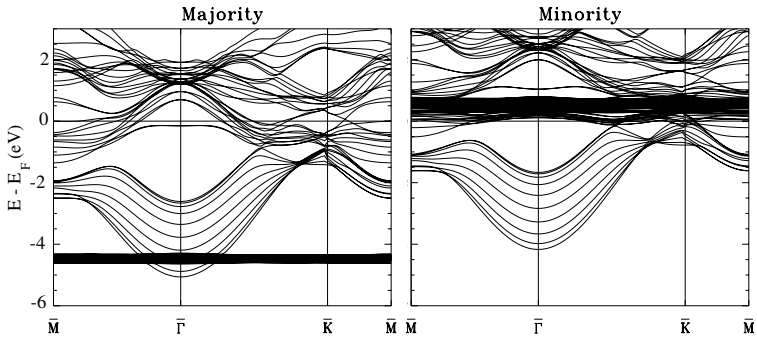

Figure 7. LDA band structure of the Gd(0001) surface, calculated within the 4f-band model at the theoretical lattice constant including the relaxation of the surface. The majority spin states are shown in the left-hand panel and the minority states in the right-hand panel.

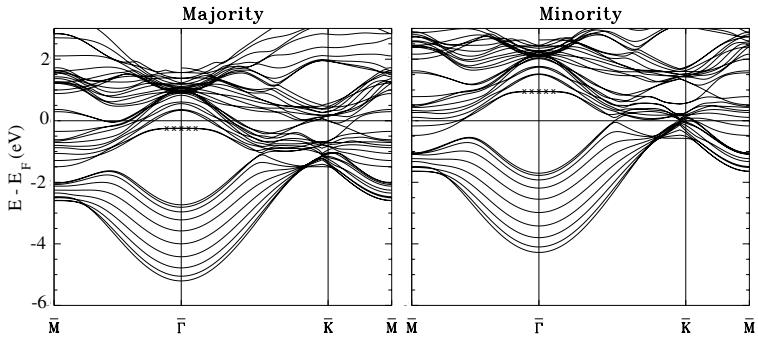

Figure 8. LDA band structure of the Gd(0001) surface, calculated within the 4f-core model at the theoretical lattice constant including the relaxation of the surface. The majority spin states are shown in the left-hand panel and the minority states in the right-hand panel. The surface states around the $\overline{\Gamma}$-point are marked with small crosses.

Figure 8 shows the band structure obtained within the 4f-core model. The 4f states that are clearly visible in figure 7 have been removed from the valence band region. Similar to the bulk case the main difference between the two models to treat the 4f electrons is a shift of the Fermi energy. At the surface this shift amounts to about 0.1 eV. Thus, at the $\overline{\Gamma}$-point the majority and minority parts of the surface state (marked with small crosses in figure 8) are now found at 0.24 eV below and 0.95 eV above the Fermi energy, respectively. The spin splitting of the surface state remains unchanged. Hence, the binding energy of the majority part of the surface state is now in even better agreement with experiment. However, the minority part is still found about 0.40 eV higher than observed experimentally. As said above the surface state is mostly localized in the surface and vacuum region, which causes the interaction with the Gd substrate to be small. This argument is further substantiated by the very small dependence of the binding energy of the minority and majority parts of the surface state upon the interlayer relaxation. In the ideal bulk truncated structure the energetic positions of the majority and the minority surface states are at 0.22 eV below and 0.98 eV above the Fermi energy, respectively. However, the dependence on the in-plane lattice constant could be different. Therefore, we have repeated the LDA 4f-core model calculation on the experimental lattice constant using the calculated inwards relaxation of 2.9% for the surface layer. The experimental in-plane lattice constant is 1.4% larger than the theoretical LDA 4f-core equilibrium lattice constant.

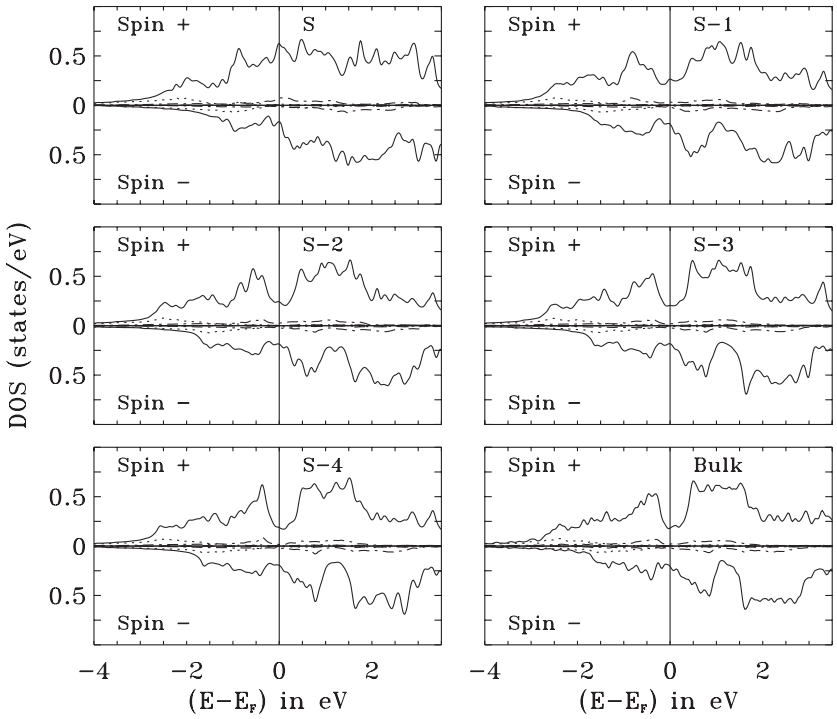

Figure 9. DOS due to s (dotted), p (dash–dotted) and d (solid curve) electrons inside the muffin-tin spheres of the different layers (S = surface, $S-1$ = subsurface, ...) of a ten-layer Gd(0001) film, calculated using the LDA 4f-core model. The density of bulk hcp Gd has been added for comparison.

Using the experimental lattice constant the majority and minority parts of the surface state at the $\overline{\Gamma}$-point are found at 0.21 eV below and 0.98 eV above the Fermi energy, respectively. Hence, the variation of the binding energy with changing in-plane lattice constant is also small. The application of the LDA + U model also brought no significant change of the results: at the $\overline{\Gamma}$-point the surface states are located 0.22 eV below and 0.92 eV above E_F.

To sort out possible errors for the binding energy for the minority surface state we calculated the Gd(0001) surface with an fcc stacking fault in the first layer. Even this changed the energetic positions only to −0.16 eV and 0.99 eV relative to E_F for the majority and minority surface states, respectively. This shows once more that the surface state is well localized in the first layer. Nevertheless it should be noticed that the formation of an fcc stacking fault at the surface is energetically unfavourable. We calculated a formation energy of 57 meV per stacking fault. Since the results were found to depend little on the relaxations and lattice constant, the following results are presented using the experimental lattice constant and the calculated inwards relaxation of 2.9% for the surface layer.

4.4. Density of states and STS spectra

The DOS obtained from the LDA 4f-core calculation is presented in figure 9 for all atoms in the film. It can clearly be seen that the main contribution to the DOS originates from d electrons. Moving from the surface (S) to the subsurface layer ($S-1$) the DOS changes rapidly, becoming more and more bulklike. The DOSs of the inner ($S-2$, $S-3$, $S-4$) layers of the film are very

similar to the bulk DOS. The bulk majority DOS shows a pronounced depression (pseudo-bandgap) at the Fermi energy. Due to the spin splitting the minority counterpart of this gap is found about 1.2 eV above the Fermi energy. The two spin components of the surface state fall exactly into this energy region (cf figure 8). The DOS due to the surface state fills these gaps. Consequently, these gaps are not visible in the DOS of the surface layer. However, in the subsurface layer the gaps are already clearly visible, which shows again the strong surface localization of the surface state.

In recent years the surface of Gd(0001) has been extensively studied by STS [49]. This method offers the possibility of measuring the occupied and unoccupied surface states. In these experiments two pronounced peaks at -0.22 and 0.49 eV (relative to E_F) have been found, which were identified as occupied majority and unoccupied minority surface states. Spin-polarized STS [50] confirms this assumption.

Motivated by this new development, we investigate the STS spectrum within the Tersoff–Hamann model [51]. In this model, the tunnelling current of a scanning tunnelling microscope (STM) is proportional to the spin-integrated local density of states (LDOS) of the sample at the position of the tip [52], while in a spin-polarized STM it is proportional to the spin-resolved LDOS. The majority (minority) LDOS in the vacuum region of the Gd(0001) film is shown in blue (green) in figure 10 for several distances from the surface layer. The two spin components of the surface state are clearly visible as two pronounced peaks in the majority and minority LDOS respectively. These peaks are directly observed in an STS experiment (e.g. [48]), which probes the total LDOS. However, as we have pointed out before, the minority peak is found much closer to the Fermi energy experimentally than in our calculation. Figure 10 also contains density plots of both the occupied majority surface state and its unoccupied minority counterpart. From this plot the surface state can be identified as a d_{z^2} state. The strong surface localization is also clearly visible. A large fraction of the charge density of the surface state is found above the surface layer.

5. Summary

We investigated bulk hcp Gd and the Gd(0001) surface, treating the 4f states in different models: LDA and GGA, 4f as valence and core states, using LDA + U and the hybrid model. In all cases, a description of the 4f electrons as valence electrons (without an extension such as LDA + U or the hybrid model) using the LDA or GGA exchange–correlation functionals led to qualitatively wrong results: bulk hcp Gd was AFM and the surface layer of the Gd(0001) surface showed only a small tendency towards FM coupling to the bulk layers. Using the 4f-core model (or any other model that removes the minority 4f states from the Fermi level, such as the LDA + U or the hybrid model), we found FM order for bulk and surface. We discussed the Curie temperatures of these systems and found lattice constants and surface relaxations in good agreement with the experiment. The enhancement of the surface magnetic moment and a simulated STS spectrum of the spin-split surface state of Gd(0001) are in qualitative agreement with experimental data. The binding energy of the occupied 5d majority surface state is in good agreement with the experimental value, while the unoccupied minority surface state was found about 0.4 eV too high in energy.

Acknowledgments

The authors thank Alexander B Shick for his help in dealing with the LDA + U formalism. We thank Lars Nordström, Walter M Temmerman and Warren E Pickett for interesting and

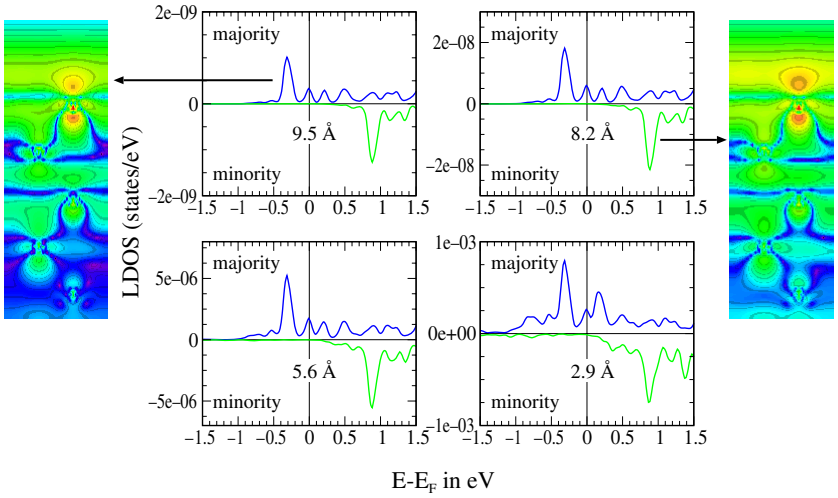

Figure 10. Local spin-resolved density of states (LSDOS) in the vacuum region calculated at different distances (2.9–9.5 Å) from the surface layer of a ten-layer Gd(0001) film, using the LDA 4f-core model. The majority (minority) LDOS is shown in blue (green). Plots of the charge density of the occupied majority and unoccupied minority surface states in a plane perpendicular to the surface are shown in the right- and left-hand panel, respectively. The plots are a cut through the upper half of the film, cutting five Gd atoms. Areas of high charge density are shown in red; low-density regions are coloured in blue.

clarifying discussions. The work was supported by the TMR Network, contract no FMRX-CT98-0178.

References

[1] Fähnle M, Hummler K, Liebs M and Beuerle T 1993 *Appl. Phys.* A **57** 67
[2] White R M 1985 *Science* **229** 11
[3] Jensen J and Mackintosh A K 1991 *Rare Earth Magnetism* (Oxford: Oxford University Press)
[4] Nordström L and Mavromaras A 2000 *Europhys. Lett.* **49** 775
[5] Koelling D D and Harmon B N 1977 *J. Phys. C: Solid State Phys.* **10** 3107
[6] Sticht J and Kübler J 1985 *Solid State Commun.* **53** 529
[7] Krutzen B C H and Springelkamp F 1989 *J. Phys.: Condens. Matter* **1** 8369
[8] Bylander D M and Kleinman L 1994 *Phys. Rev.* B **49** 1608
[9] Bylander D M and Kleinman L 1994 *Phys. Rev.* B **50** 1363
[10] Bylander D M and Kleinman L 1994 *Phys. Rev.* B **50** 4996
[11] Shick A B, Liechtenstein A I and Pickett W E 1999 *Phys. Rev.* B **60** 10 763
[12] Shick A B, Pickett W E and Fadley C S 2000 *Phys. Rev.* B **61** 9213
[13] Dimmock J O and Freeman A J 1964 *Phys. Rev. Lett.* **13** 750
[14] Ahuja R, Wills J M, Johansson B and Eriksson O 1993 *Phys. Rev.* B **22** 16 269
[15] Singh D J 1991 *Phys. Rev.* B **44** 7451
[16] Schirber E, Schmidt F A, Harmon B N and Koelling D D 1976 *Phys. Rev. Lett.* **36** 448
[17] Mattocks P G and Young R C 1977 *J. Phys. F: Met. Phys.* **7** 1219
[18] Ahuja R, Auluck S, Johansson B and Brooks M S S 1994 *Phys. Rev.* B **50** 5147
[19] Wu R, Li C, Freeman A J and Fu C L 1991 *Phys. Rev.* B **44** 9400
[20] Weller D, Alvarado S F, Gudat W, Schröder K and Campagna M 1985 *Phys. Rev. Lett.* **54** 1555
[21] Heinemann M and Temmerman W M 1994 *Phys. Rev.* B **49** 4348
[22] Heinemann M and Temmerman W M 1994 *Surf. Sci.* **307–9** 1121
[23] Lang J K, Baer Y and Cox P A 1977 *J. Phys. F: Met. Phys.* **7** 1219
[24] Quinn J, Li Y S, Jona F and Fort D 1992 *Phys. Rev.* B **46** 9694

[25] Eriksson O, Ahuja R, Ormeci A, Trygg J, Hjortstam O, Söderlind P, Johansson B and Wills J M 1995 *Phys. Rev.* B **52** 4420
[26] Anisimov V I, Aryasetiawan F and Lichtenstein A I 1996 *J. Phys.: Condens. Matter* **9** 767
[27] Tang H, Weller D, Walker T G, Scott J C, Chappert C, Hopster H, Pang A W, Dessau D S and Pappas D P 1993 *Phys. Rev. Lett.* **71** 444
[28] Vescovo E, Carbone C and Rader O 1993 *Phys. Rev.* B **48** 7731
[29] Weschke E, Schlüssler-Langeheine C, Meier R, Fedorov A V, Starke K, Hübinger F and Kaindl G 1996 *Phys. Rev. Lett.* **77** 3415
[30] Tober E D, Palomares F J, Ynzunza R X, Denecke R, Morais J, Wang Z, Bino G, Liesegang J, Hussain Z and Fadley C S 1998 *Phys. Rev. Lett.* **81** 2360
[31] Wimmer E, Krakauer H, Weinert M and Freeman A J 1981 *Phys. Rev.* B **24** 864
[32] Weinert M, Wimmer E and Freeman A J 1982 *Phys. Rev.* B **26** 4571
[33] Moruzzi V L, Janak J F and Williams A R 1978 *Calculated Electronic Properties of Metals* (New York: Pergamon)
[34] Perdew P and Wang Y 1991 *Electronic Structure of Solids* (Berlin: Akademie) vol 11
[35] Banister J R, Legvold S and Spedding F H 1954 *Phys. Rev.* **94** 1140
[36] Temmerman W M and Sterne P A 1990 *J. Phys.: Condens. Matter* **2** 5529
[37] Singh D J 1991 *Phys. Rev.* B **43** 6388
[38] Mulhollan G A, Garrison K and Erskine J L 1992 *Phys. Rev. Lett.* **69** 3240
[39] Giergiel J, Pang A W, Hopster H, Guo X, Tong S Y and Weller D 1995 *Phys. Rev.* B **51** 10 201
[40] Jenkins A C, Temmerman W M, Ahuja R, Eriksson O, Johansson B and Wills J 2000 *J. Phys.: Condens. Matter* **12** 10 441
[41] Ozoliņš V and Körling M 1993 *Phys. Rev.* B **48** 18 304
[42] Singh D J, Pickett W E and Krakauer H 1991 *Phys. Rev.* B **43** 11 628
[43] Terakura K, Hamada N, Oguchi T and Asada T 1982 *J. Phys. F: Met. Phys.* **12** 1661
[44] Rushbrook G S and Wood P J 1958 *Mol. Phys.* **1** 257
[45] Jenkins A C and Temmerman W M 1999 *J. Magn. Magn. Mater.* **198–9** 567
[46] Asato M, Settels A, Hoshino T, Asada T, Blügel S, Zeller R and Dederichs P H 1999 *Phys. Rev.* B **60** 5202
[47] Arnold C S and Pappas D P 2000 *Phys. Rev. Lett.* **85** 5202
[48] Getzlaff M, Bode M, Heinze S, Pascal R and Wiesendanger R 1998 *J. Magn. Magn. Mater.* **184** 155
[49] Getzlaff M, Bode M, Heinze S and Wiesendanger R 1999 *Appl. Surf. Sci.* **142** 558
[50] Bode M, Getzlaff M and Wiesendanger R 1999 *J. Vac. Sci. Technol.* A **17** 2228
[51] Tersoff J and Hamann D 1983 *Phys. Rev. Lett.* **50** 1998
[52] Heinze S, Blügel S, Pascal R, Bode M and Wiesendanger R 1998 *Phys. Rev.* B **58** 16 432